Int. J. Electrochem. Sci., 16 **(2021)** Article ID: 210916, doi: 10.20964/2021.09.36

International Journal of
ELECTROCHEMICAL
SCIENCE
www.electrochemsci.org

Study on the Corrosion Inhibition Performance of a Schiff Base for Carbon Steel in 1 M HCl Solution

Xiumei Wang[*], *Jiani Xing and Zongquan Huang*

Shenyang Jianzhu University, Shenyang, 100168, China
[*]E-mail: xmwang@alum.imr.ac.cn

Received: 17 May 2021 / *Accepted:* 9 July 2021 / *Published:* 10 August 2021

To investigate the corrosion of carbon steel in acidic media, weight loss measurements, electrochemical methods, thermodynamic adsorption isotherms and scanning electron microscopy (SEM) observations were adopted to study the Schiff base N,N'-bis(4-hydroxy-benzylidene)-triethylenetetramine (N,N'-BHMTT) as a corrosion inhibitor for carbon steel in 1 M HCl. The corrosion inhibitor exhibited excellent performance. The corrosion inhibition efficiency was as high as 82.5% at 25 mg L^{-1} N,N'-BHMTT (weight loss result). The corrosion inhibitor simultaneously slowed the cathodic and anodic corrosion processes of carbon steel. N,N'-BHMTT is a mixed corrosion inhibitor with an almost unchanged corrosion potential. The adsorption of N,N'-BHMTT on the surface of carbon steel obeyed the Langmuir adsorption isotherm along with a mixture of physical and chemical adsorption, forming a complete and dense protective film on the carbon steel surface that acted as a barrier to inhibit corrosive media from effectively contacting the carbon steel surface.

Keywords: corrosion, carbon steel, 1 M HCl solution, corrosion inhibitor, Schiff base

1. INTRODUCTION

In many industrial fields, anticorrosion technology for metals is of great significance. Among anticorrosion technologies, corrosion inhibitors are widely used in oilfield mining, chemical cleaning, sewage processing and other fields as an efficient and convenient anticorrosion method. The addition of corrosion inhibitors to acidic media is one of the most practical methods to prevent metals from corrosion. Inorganic corrosion inhibitors are banned due to their high toxicity. In recent years, organic corrosion inhibitors have attracted the interest of researchers. According to the structure-activity relationship, organic compounds containing heteroatoms such as N, O, S, P and aromatic rings, unsaturated bonds or π electrons exhibit good corrosion inhibition properties [1-6]. Schiff bases have been studied as corrosion inhibitors due to their low cost, easy synthesis, nontoxicity and high corrosion inhibition [7-16]. Schiff bases are compounds obtained by condensation reactions of amines

and active carboxides, such as aldehydes or ketones. Schiff base molecules contain a special functional group C=N, which can be strongly attached to a metal surface to prevent metal corrosion by multiple active adsorption modes. Among the studies on Schiff bases, the use of N,N'-bis(4-hydroxy-benzylidene)-triethylenetetramine (N,N'-BHMTT) as a corrosion inhibitor has not been reported. N,N'-BHMTT is expected to behave as an excellent corrosion inhibitor for metals due to the multiple N and O heteroatoms and delocalized π electrons in its structure. In this paper, Schiff base N,N'-BHMTT was synthesized, and static weight loss measurements, electrochemical tests and scanning electron microscopy (SEM) observations were used to investigate its corrosion inhibition performance and mechanism when protecting carbon steel in 1 M HCl.

2. EXPERIMENT

2.1 Synthesis of Schiff base corrosion inhibitor

Briefly, 4-hydroxybenzaldehyde (20 mmol) was dissolved in 10 mL of absolute ethanol. Both triethylenetetramine (10 mmol) and 5 drops of glacial acetic acid were dissolved in 5 mL of absolute ethanol to be used as a catalyst. A yellow precipitate was obtained by dropwise adding the 4-hydroxybenzaldehyde solution into the triethylenetetramine solution at room temperature with electromagnetic stirring. The dropwise addition was controlled to be completed in 30 min. After that, the mixture was stirred for 2 h and refluxed at 80 °C for 4 h. Then, the sample was filtered to collect the solid product, which was washed with diethyl ether three times, recrystallized with absolute ethanol, and finally dried to obtain a pure yellow powder product (yield of 78.7%, M.P. 120 °C). The synthesis route and structure of the corrosion inhibitor N,N'-BHMTT are shown in Scheme 1 and Figure 1, respectively.

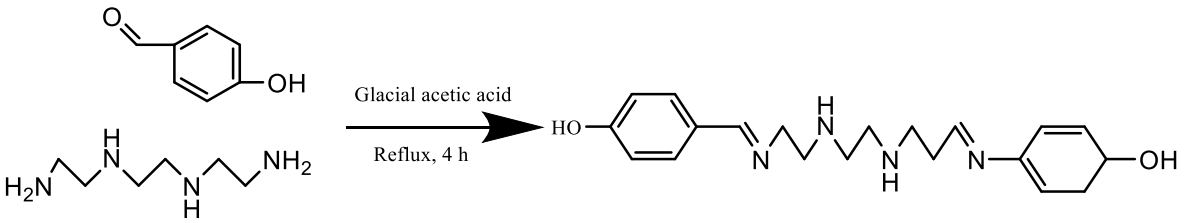

Scheme 1. Synthesis route of N,N'-BHMTT.

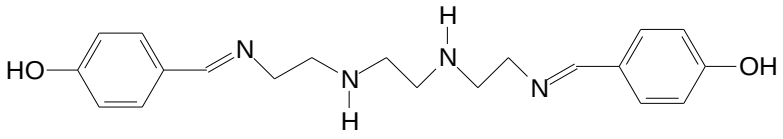

Figure 1. Chemical structure of N,N'-BHMTT.

2.2 Weight loss measurements

Weight loss experiments were conducted according to the standard method [17]. Carbon steel specimens with dimensions of 20 mm×20 mm×10 mm were successively abraded with #100~1200 emery papers to obtain bright surfaces. Then, these specimens were washed with distilled water, degreased with absolute ethanol, dried with dry air and stored in a vacuum desiccator. After being accurately weighed with a high sensitivity balance (±0.1 mg) and measured with a Vernier caliper (sensitivity of ±0.01 mm), the specimens were immersed in 200 mL of 1 M HCl with and without various concentrations (25, 50, 100, 200 mg L^{-1}) of N,N'-BHMTT at 30 °C under aerated conditions for 4 h. After 4 h of immersion, the specimens were removed, rinsed thoroughly with running water, scrubbed with alcohol cotton, and dried with dry air, before being weighed and accurately measured again. The weight loss measurement for each concentration was conducted in triplicate. At 200 mg L^{-1}, the inhibition efficiency versus immersion time (4 h, 6 h, 8 h, and 10 h) was determined according to the above weight loss experimental procedure, including carbon steel polishing, immersion and posttreatment. The corrosion rate (V) and inhibition efficiency (IE, %) were calculated by equations (1) and (2):

$$V = \frac{\Delta m}{S \cdot \Delta t} \quad (1)$$

$$IE(\%) = \frac{V' - V}{V'} \times 100\% \quad (2)$$

where Δm is the average weight loss of the carbon steel in three parallel experiments, g; S is the average total surface area of the specimens, m^2; t is the immersion time, h; and V' and V are the values of the corrosion rate without and with the addition of corrosion inhibitor, respectively, g $m^{-2} \cdot h^{-1}$.

2.3 Surface morphological studies

The change in the morphology of the carbon steel surface was studied by obtaining images of the carbon steel specimens before and after immersion in 1 M HCl without and with 200 mg L^{-1} N,N'-BHMTT for 4 h at 30 °C using a scanning electron microscope (Hitachi S-4800) with an accelerating voltage of 15 kV at a magnification of 3000×. The dimensions and treatment of the carbon steel specimens for the SEM study were the same as those for the weight loss measurement.

2.4 Electrochemical measurements

Electrochemical measurements were performed using a computer-controlled electrochemical workstation (PARSTAT2273, USA). A three-electrode system consisting of a carbon steel specimen as the working electrode, a platinum electrode as the counter electrode and a saturated calomel electrode (SCE) as the reference electrode was used. The carbon steel electrode was sealed with epoxy resin except for the working surface (1 cm^2). The working surface was gradually abraded with #100~1200 emery papers, washed, degreased and dried before use. Before measurement, the working electrodes were immersed in the corrosive solution for approximately 30 min until the open circuit potential (OCP) reached a steady state. Electrochemical impedance spectroscopy (EIS) tests were performed in

a frequency range of 100 kHz to 0.01 Hz with an amplitude of 10 mV at the open circuit potential. The potentiodynamic polarization curves were recorded on the same electrode by changing the voltage from -0.15~+0.25 V with respect to the open circuit potential (OCP) at a scan rate of 0.005 V s^{-1}. All potentials were measured in this study as references to the SCE. The potentiodynamic polarization curve and EIS results were analyzed by PowerSuite and ZSimpWin software. The acquired parameters i_{corr} (current density) and R_{ct} (charge transfer resistance) were used to calculate the inhibition efficiency (*IE*, %) by the following (equations (3) and (4)):

$$IE(\%) = \frac{i^0_{corr} - i_{corr}}{i^0_{corr}} \times 100\% \quad (3)$$

where i^0_{corr} and i_{corr} are the corrosion current densities of the carbon steel electrodes in the uninhibited and inhibited solutions, A cm^{-2}; and

$$IE(\%) = \frac{R_{ct} - R^0_{ct}}{R_{ct}} \times 100\% \quad (4)$$

where R^0_{ct} and R_{ct} are the charge transfer resistances of the carbon steel electrodes in the uninhibited and inhibited solutions, Ω cm^2.

3. RESULTS AND DISCUSSION

3.1 Weight loss results

The inhibition efficiency values of N,N'-BHMTT with different concentrations for carbon steel in 1 M HCl are shown in Figure 2(a). It is obvious that the inhibition efficiency increases with the increase in the studied concentration range of N,N'-BHMTT in 1 M HCl. The inhibition efficiency of N,N'-BHMTT was over 80%, even at 25 mg L^{-1}. This phenomenon can be attributed to the strong interaction of the N,N'-BHMTT molecule with the carbon steel surface due to adsorption [18]. The extent of adsorption of the N,N'-BHMTT molecule on the carbon steel surface increases with the increase in the concentration of N,N'-BHMTT, resulting in a higher inhibition efficiency, and the maximum inhibition efficiency value occurs with 200 mg L^{-1} N,N'-BHMTT. These results are due to an increase in the number of N,N'-BHMTT molecules adsorbed on the carbon steel surface. Thus, more of the active sites of carbon steel are covered by N,N'-BHMTT molecules, which decreases the corrosion rate. In general, organic compounds inhibit metal dissolution by forming a protective film on the metal surface and separating it from the corrosive medium [19–22]. The good corrosion inhibition ability of N,N'-BHMTT depends on the strong chemical bonds among Fe atoms and the lone pair of electrons present on N atoms and π electrons present in the >C=N- moiety and benzene ring. The variation in the corrosion inhibition efficiency of 200 mg L^{-1} N,N'-BHMTT against immersion time is presented in Figure 2b. The increase in immersion time from 4 to 10 h did not cause any significant change in inhibition efficiency (95.0, 96.1, 96.5, 95.5%), thereby suggesting that N,N'-BHMTT is an effective corrosion inhibitor for up to 10 h of immersion [23]. This result is due to the stable adsorption of inhibitor on the carbon steel surface.

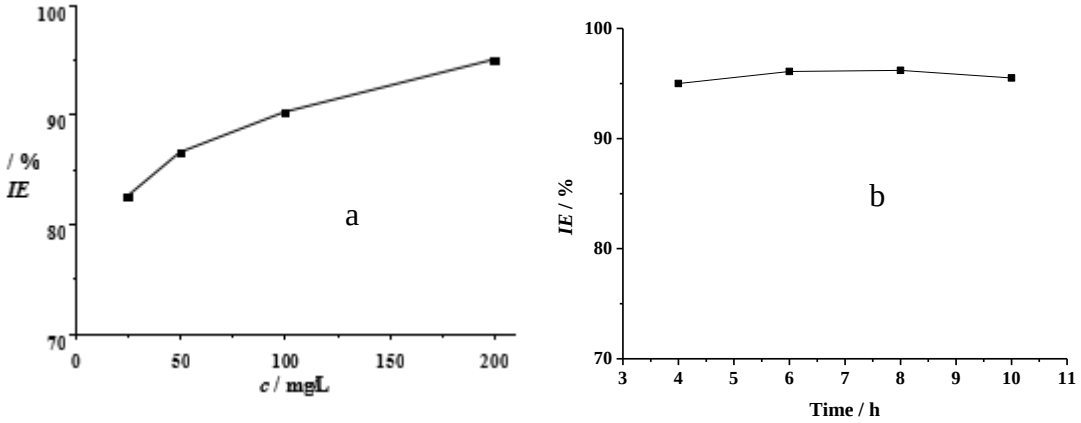

Figure 2. Effects of the N,N'-BHMTT concentration (a) and immersion time (4 h, 6 h, 8 h, 10 h) with 200 mg L^{-1} N,N'-BHMTT (b) on the inhibition efficiency of N,N'-BHMTT for protecting carbon steel in 1 M HCl.

3.2 Electrochemical Results

3.2.1 Polarization curves

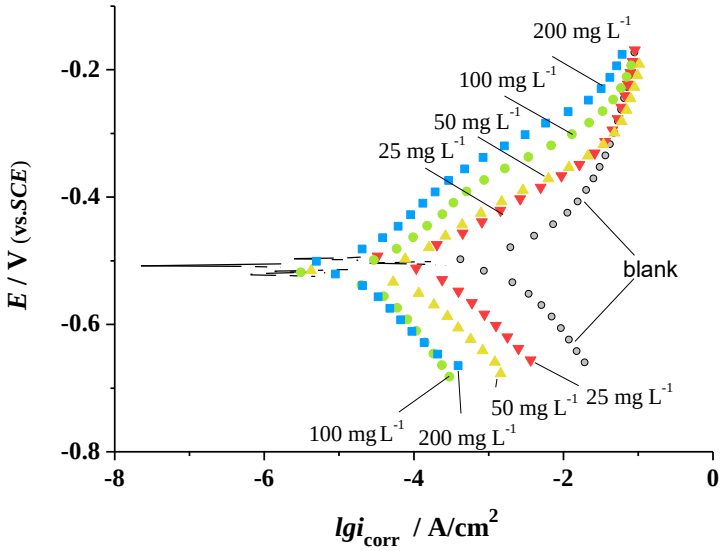

Figure 3. Polarization curves of carbon steel in 1 M HCl without and with different concentrations of corrosion inhibitor.

The polarization curve of carbon steel immersed in corrosion solution for 0.5 h at 30 °C was obtained and is displayed in Figure 3.

Figure 3 shows that the corrosion current density of carbon steel immersed in inhibited solution decreases drastically compared to that of carbon steel immersed in uninhibited solution, implying that the corrosion inhibitor suppresses carbon steel corrosion. Both anodic and cathodic polarization curves

shift to lower current densities, signifying that anodic and cathodic corrosion processes are simultaneously inhibited. The corrosion current density decreases and the corrosion inhibition efficiency increases gradually as the concentration is increased. This is due to the inhibitor molecules forming a dense and compact adsorption film on the carbon steel surface, which separates the carbon steel from the corrosive solution. The obtained electrochemical parameters (E_{corr}, i_{corr}, etc.), which were obtained by the extrapolation method from the polarization curves, and the inhibition efficiency (*IE*, %), which was calculated according to equation (3), are listed in Table 1.

Table 1. Parameters of the polarization curves of carbon steel in 1 M HCl with different concentrations of corrosion inhibitor by the extrapolation method.

C / mg L^{-1}	$-E_{corr}$ / V vs SCE	ΔE_{corr} / V	i_{corr} / A cm^{-2}	*IE* / %
blank	0.504	--	1.69×10^{-5}	--
25	0.497	0.007	1.17×10^{-5}	30.8
50	0.516	-0.012	5.12×10^{-6}	69.8
100	0.522	-0.018	3.01×10^{-6}	82.2
200	0.508	-0.004	3.89×10^{-7}	97.7

$\Delta E_{corr}=E_{corr}-E^0_{corr}$, where E_{corr} and E^0_{corr} are the self-corrosion potentials of carbon steel immersed in inhibited solution and uninhibited solution, respectively.

From Table 1, there are no distinct changes in the E_{corr} value while the i_{corr} value of the inhibited solution decreases compared to the blank corrosive solution. The maximum value of ΔE_{corr} is 18 mV (<85 mV), indicating that N,N'-BHMTT is a mixed corrosion inhibitor [3]. Both cathodic hydrogen evolution and anodic dissolution processes are inhibited. The adsorbed film of N,N'-BHMTT on the carbon steel surface becomes more compact with increasing inhibitor concentration, which prevents more of the corrosive solution from reaching the carbon steel surface; thus, the inhibition efficiency increases correspondingly.

3.2.2 EIS results

The Nyquist plots of the carbon steel specimens immersed in corrosion solution for 0.5 h at 30 °C were obtained and are depicted in Figure 4. The shape of the Nyquist plot of the carbon steel electrode remains unchanged by the addition of inhibitor. This phenomenon indicates that the inhibitor does not change the mechanism of carbon steel corrosion.

The characteristic of a semicircular capacitive arc with one time constant indicates that metal dissolution is only controlled by the charge transfer process [24]. The imperfect semicircular capacitive arcs are due to the frequency dispersion caused by the roughness and inhomogeneity of the electrode surface. A significant increase in the radius of the capacitive arc of the carbon steel electrodes can be observed in Figure 4 after the addition of N,N'-BHMTT in 1 M HCl, suggesting that the impedance

values increase. Furthermore, the impedance value increases with increasing concentrations of corrosion inhibitor. The increase in impedance may be due to the formation of a more complete N,N'-BHMTT film, causing fewer electron transfer processes to occur on the carbon steel surface. The equivalent circuit shown in Figure 5 is used to fit the Nyquist plots. R_{ct} is the charge transfer resistance, *CPE* is the constant phase element instead of pure electric double layer capacitance, and R_s is the solution resistance. The obtained electrochemical parameters [25, 26] obtained by fitting the Nyquist plots and the calculated inhibition efficiency (*IE*, %) by R_{ct} are displayed in Table 2. As the concentration of corrosion inhibitor increases, *CPE* decreases and R_{ct} increases. The decrease in *CPE* is due to the decrease in the dielectric constant or the increase in the thickness of the electric double layer due to more corrosion inhibitor molecules with lower dielectric constants displacing the water molecules and other particles that were originally adsorbed at the carbon steel-solution interface. *IE* increases with increasing corrosion inhibitor concentration and reaches 95.0% at 200 mg L^{-1}.

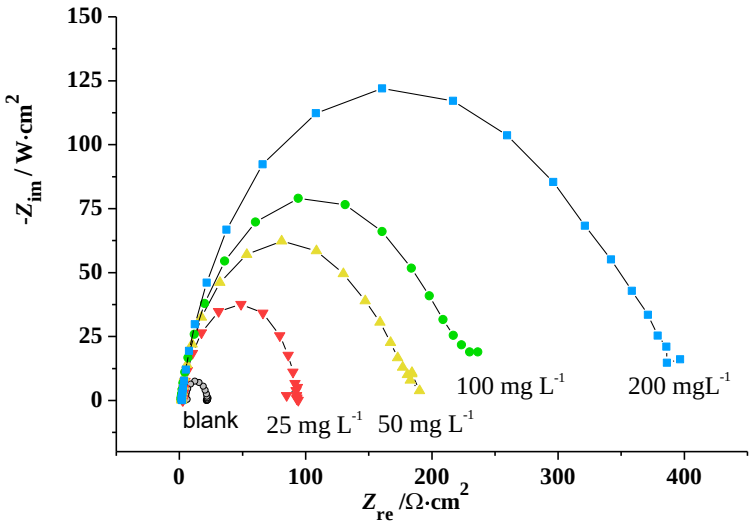

Figure 4. Nyquist plots of carbon steel in 1 M HCl without and with different concentrations of corrosion inhibitor.

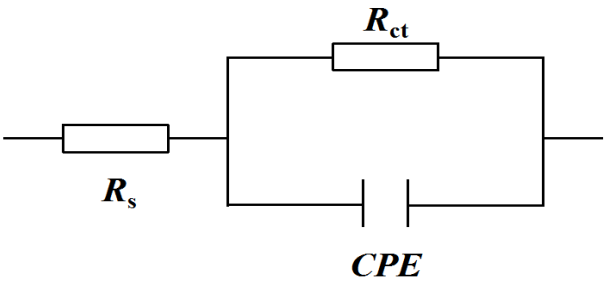

Figure 5. Equivalent circuit.

Table 2. Fitted parameters of the Nyquist plots of carbon steel in 1 M HCl with different doses of corrosion inhibitor.

C / mg L^{-1}	R_s / Ω cm^2	*CPE* /μF cm^{-2}	R_{ct} / Ω cm^2	*IE* / %
blank	1.8	873	20	--
25	2.4	332	79	74.6
50	2.0	289	178	88.7
100	2.1	173	237	91.5
200	2.0	86	402	95.0

3.3 SEM Results

The SEM results of carbon steel specimens immersed in blank HCl solution and in HCl with the addition of 200 mg L^{-1} N,N'-BHMTT are shown in Figure 6. Figure 6a shows that the carbon steel surface is uneven accompanied with some pits and bumps, indicating that the carbon steel specimen suffers from severe corrosion. Compared to Figure 6a, Figure 6b shows that the carbon steel surface is very smooth. Moreover, the original scratches polished by emery paper on the carbon steel surface are clearly observed, suggesting that the addition of corrosion inhibitor greatly impedes the carbon steel from corrosion in 1 M HCl. This result is due to the decrease in the number of active sites on the carbon steel surface caused by the corrosion inhibitor film covering the carbon steel surface.

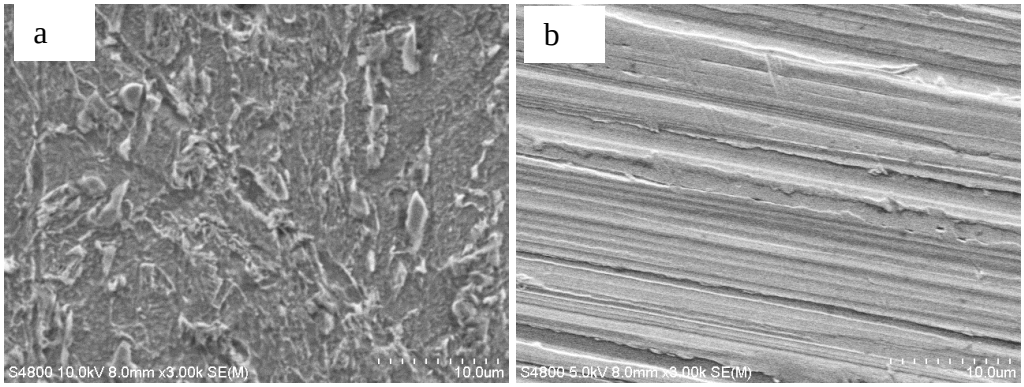

Figure 6. SEM images of the carbon steel specimens immersed in 1 M HCl: (a) blank and (b) with 200 mg L^{-1} N,N'-BHMTT.

3.4 Adsorption isotherm

The corrosion inhibition mechanism of organic corrosion inhibitors proposes that organic molecules are adsorbed on the metal surface by displacing the already adsorbed water molecules to form a dense and complete barrier film, thus covering the active sites of carbon steel and inhibiting corrosion.

In view of the fact that N,N'-BHMTT is a mixed corrosion inhibitor, the surface coverage θ is numerically equal to the corrosion inhibition efficiency. From the weight loss data, the coverage θ can be calculated by equation (5):

$$\theta = \frac{V' - V}{V'} \quad (5)$$

where V' and V are the corrosion rates of the carbon steel in 1 M HCl without and with different concentrations of N,N'-BHMTT, g $m^{-2} \cdot h^{-1}$.

Substituting the calculated coverage θ into different adsorption isotherms, it is found that the data fit the Langmuir isotherm very well. The Langmuir isotherm is as follows (equation (6)):

$$\frac{c}{\theta} = \frac{1}{K} + c \quad (6)$$

where K is the adsorption equilibrium constant, L g^{-1}; c is the corrosion inhibitor concentration (mg L^{-1}); and θ is the surface coverage (calculated from the weight loss data),

The result obtained by plotting c/θ vs. c is depicted in Figure 7, and the fitting parameters are listed in Table 3. Figure 7 and Table 3 show that the plot of c/θ vs. c is a straight line with a linear correlation coefficient that is close to 1 and a slope that is near unity, indicating that the adsorption of N,N'-BHMTT on the carbon steel surface obeys the Langmuir adsorption isotherm. The small deviation from unity in the slope may be due to attractive or repulsive forces among the N,N'-BHMTT molecules adsorbed on the carbon steel surface [27-28]. The K value can be calculated by the intercept of the plot of c/θ vs. c, and the corresponding result is 163 L g^{-1}.

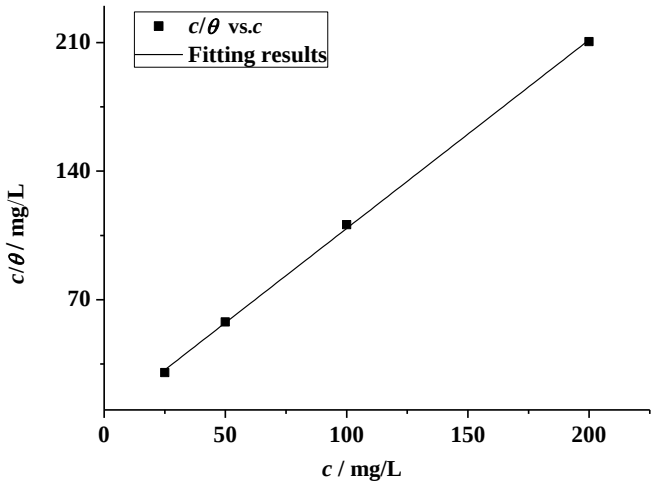

Figure 7. Langmuir isotherm and the fitting results of the corrosion inhibitor on the carbon steel surface (θ is obtained from the weight loss results).

$$\Delta G° = -RT\ln 10^6 K \quad (7)$$

In the above equation, R represents the molar gas constant, 8.314 J mol^{-1} K^{-1}; T represents the absolute temperature, K; ΔG^o denotes the adsorption Gibbs free energy, kJ mol^{-1}; and K is the adsorption equilibrium constant, L g^{-1}.

The value of Gibbs free energy ΔG^o is an important parameter to describe the adsorption process of corrosion inhibitors. In general, it is believed that a negative ΔG^o value indicates a spontaneous adsorption process. A negative ΔG^o value of approximately -20 kJ mol^{-1} or lower is regarded as physical adsorption (electrostatic attraction forces) between charged corrosion inhibitor molecules and the charged metal surface, while those of approximately -40 kJ mol^{-1} or higher are considered chemical adsorption, in which the electrons of the corrosion inhibitor molecules are shared or transferred. The negative ΔG^o value between -20~-40 kJ mol^{-1} is associated with the combination of physical adsorption and chemical adsorption. In our work, the calculated ΔG^o value is -30.3 kJ mol^{-1}, indicating that the adsorption of corrosion inhibitor on the carbon steel surface is a spontaneous and mixed adsorption process that consists of physical and chemical adsorption.

3.5 Inhibition mechanism

From the above results obtained from the electrochemical tests, weight loss measurements and SEM images, it was concluded that N,N'-BHMTT as a corrosion inhibitor suppresses the corrosion of carbon steel in 1 M HCl through a combination of physical and chemical adsorption on the carbon steel surface. In 1 M HCl, the carbon steel surface is positively charged, and N,N'-BHMTT can be easily protonated due to its N atoms. The inhibition mechanism of N,N'-BHMTT against carbon steel corrosion is as follows: (1) electrostatic interaction between protonated molecules and the excessive Cl^- ions adsorbed on carbon steel surface (physical adsorption), (2) donor–acceptor interactions between the π electrons of the aromatic ring and the vacant d-orbital of the iron atoms (chemical adsorption), and (3) interaction between the unshared electron pairs of N and O and the vacant d-orbital of the iron atoms on the surface (chemical adsorption) [29]. N,N'-BHMTT is a kind of bis-Schiff base with multiple heteroatoms, two C=N bonds and two benzene rings. The C=N bonds with a relatively high electron cloud density and the large delocalized π bonds with multiple active sites can provide electrons to the inner d orbitals of Fe atoms to form stable multicenter adsorption through stable coordination bonds. Thus, the adsorption film is more stable, compact and difficult to desorb from the carbon steel surface, leading to its excellent inhibition efficiency. Both physical adsorption (ionic adsorption) and chemical adsorption (molecular adsorption) mechanisms stabilize the barrier film of N,N'-BHMTT formed on the carbon steel surface to effectively inhibit the corrosion of carbon steel.

Table 3. Absorption and thermodynamic parameters of the corrosion inhibitor on carbon steel in 1 M HCl.

T / ℃	R^2	Intercept	slope	K / L g^{-1}	$-\Delta G^o$ / kJ mol^{-1}
30	0.99941	6.11826	1.02673	163	30.3

4. CONCLUSION

The corrosion inhibition of N,N'-bis(4-hydroxy-benzylidene)-triethylenetetramine (N,N'-BHMTT) for carbon steel in 1 M HCl is studied, and the conclusions are drawn as follows:

(1) N,N'-BHMTT behaves as an excellent corrosion inhibitor for carbon steel in 1 M HCl at 30 °C. N,N'-BHMTT (25 mg L^{-1}) exhibits good corrosion inhibition with an inhibition efficiency of 82.5%. The inhibition efficiency increases with increasing inhibitor concentration and reaches the maximum inhibition efficiency with 200 mg L^{-1} N,N'-BHMTT. The inhibition efficiency has no obvious change over the studied immersion time, and the optimum value is 96.2% at 8 h immersion.

(2) Electrochemical results indicate that N,N'-BHMTT acts as a mixed corrosion inhibitor by inhibiting both anodic carbon steel oxidation and cathodic hydrogen reduction reactions.

(3) N,N'-BHMTT adsorption on the carbon steel surface obeys the Langmuir isotherm along with a spontaneous and mixed adsorption process (physisorption and chemisorption).

ACKNOWLEDGEMENTS
The authors gratefully acknowledge the financial support from the Liaoning Provincial Department of Education (Grant No. lnjc202016 and lnzd201905) and Xingliao Talent Program of Liaoning Province (Grant No. XLYC2002005).

References

1. A. Farhadian, A. Rahimi, NehzatSafaei, A. Shaabani, M. Abdouss, AliAlavi, *Corros. Sci*., 175 (2020) 108871.
2. A. Shamsa, R. Barker, Y. Hua, E. Barmatov, T. L. Hughes, *Corros. Sci*., 176 (2020) 108916.
3. Q. Zhao, J. X. Guo, G. D. Cui, T. Han,Y. H. Wu, *Colloids and Surf*. B, 194 (2020) 111150.
4. C. M. Fernandes, L. V. Faro, V. G. S.S.Pina, M. C. B.V. Souza, F. C.S. Boechat, M. C. Souza, M. Briganti, F. Totti, E. A. Ponzio, *Surf. Interfaces*, 21 (2020) 100773.
5. J. Haque,V. Srivastava, M. A. Quraishi, D. Chauhan, H. Lgaz, I. M. Chung, *Corros. Sci*., 172 (2020) 108665.
6. T. D. Ma, B. M. Tan,Y. Xu, D. Yin, G. R. Liu, N. Y. Zeng, G. Q. Song, Z. X. Kao, Y. L. Liu, *Colloids Surf*.A, 599 (2020) 124872.
7. K. C. Emregul, E. Duzgun, O. Atakol, *Corros. Sci*., 48 (2006) 3243.
8. H. Kele, M. Keles, I. Dehri, *Colloids Surf* A, 320 (2008) 138.
9. M. G. Hosseini, M. Ehteshamzadeh, T. Shahrabi, *Electrochim Acta*, 52 (2007) 3680.
10. K. S. Poornima, G. Parameswaran, *Corros. Sci*., 52(2010)224.
11. T. Poornima, J. Nayak, *Corros. Sci*, 53(2011)3688.
12. N. A. Negm, F. M. Ghuiba, S. M. Tawfik, *Corros. Sci*, 53 (2011) 3566.
13. M. A. Bedair, M. M. B.El-Sabbah, A. S. Fouda, H. M. Elaryian, *Corros.Sci*., 128 (2017) 54.
14. M. Murmu, S. Kr. Saha, N. C. Murmu, *Corros. Sci*., 146 (2019) 134.
15. D. Daoud, T. Douadi, S. Issaadi, S. Chafa, *Corros. Sci*., 79 (2014) 50.
16. E. Barmatov, T. Hughes, *Mater. Chem. Phys*., 257 (2021) 123758.
17. X. H. Li, S. D. Deng, H. Fu, G. N. Mu, N. Zhao, *Appl. Surf. Sci*., 254 (2008)5574.
18. G. K. Gomma, *Mater. Chem. Phys*. 55 (1998)241.
19. A. I. Onuchukwu, S. P. Trasatti, S. Trasatti, *Corros. Sci*. 36 (1994) 1815.
20. I. F. Fishtik, I. I. Vataman, F. A. Spatar, *J. Electroanal. Chem*.,165 (1984) 1.
21. S. Martinez, I. Stern, *J. Appl. Electrochem.* 31 (2001) 973.

22. S. Cheng, S. Chen, T. Liu, X. Chang, Y. Yin, *Mater. Lett*.,61 (2007) 3279.
23. I. Ahamad, M. A. Quraishi, *Corros. Sci*., 52 (2010) 651.
24. S.Sayed Abd El Rehim, A. A. Mohammed, S.O. Moussa, S. E. Abdallah, *Mater. Chem. Phys*., 112 (2008) 898.
25. A. Y. Adesina, Z. M. Gasem, K. A. Madhan, *Metall. Mater. Trans*. B, 48 (2017) 1321.
26. A. K. Singh, E. E. Ebenso, M. A. Quraishi, *Res. Chem. Intermediat*., 39 (2013) 3033.
27. A. M. Al-Sabagh, M. A. Migahed, H. S. Awad, *Corros. Sci*., 48 (2006) 813.
28. K. K. Anupama, K. Ramya, K. M. Shainy, Abraham Joseph, *Mater. Chem. Phys*., 167 (2015) 28.
29. M. A. Quraishi, D. Jamal, *Mater. Chem. Phys*., 68 (2001) 283.

© 2021 The Authors. Published by ESG (www.electrochemsci.org). This article is an open access article distributed under the terms and conditions of the Creative Commons Attribution license (http://creativecommons.org/licenses/by/4.0/).